

Dynamic instability of microtubules: effect of catastrophe-suppressing drugs

Pankaj Kumar Mishra,¹ Ambarish Kunwar,¹ Sutapa Mukherji,¹ and Debashish Chowdhury^{*1,†}

¹*Department of Physics
Indian Institute of Technology
Kanpur 208016, India.*
(Dated: January 28, 2020)

Microtubules are stiff filamentary proteins that constitute an important component of the cytoskeleton of cells. These are known to exhibit a dynamic instability. A steadily growing microtubule can suddenly start depolymerizing very rapidly; this phenomenon is known as “catastrophe”. However, often a shrinking microtubule is “rescued” and starts polymerizing again. Here we develop a model for the polymerization-depolymerization dynamics of microtubules in the presence of *catastrophe-suppressing drugs*. Solving the dynamical equations in the steady-state, we derive exact analytical expressions for the length distributions of the microtubules tipped with drug-bound tubulin subunits as well as those of the microtubules, in the growing and shrinking phases, tipped with drug-free pure tubulin subunits. We also examine the stability of the steady-state solutions.

PACS numbers: 87.10.+e, 82.35.Pq, 87.15.Rn

I. INTRODUCTION

Microtubules are filamentary proteins and constitute a major component of the cytoskeleton of the eukaryotic cells [1, 2]. The dynamic cytoskeletal scaffolding not only supports the cell architecture and gives rise to changes in the shape of the cell but the network of its constituent filamentary proteins also provides pathways for intra-cellular transport. In other words, a wide range of dynamical processes, which are essential for sustaining life, are driven by the dynamic cytoskeleton. Therefore, a clear theoretical understanding of the fundamental physical principles behind the polymerization-depolymerization dynamics of the microtubules is expected to provide deep insight into the physics of cell shape transformations, cell motility, etc. as well as mechanisms of many sub-cellular processes like, for example, chromosome segregations during mitosis (i.e., cell division).

Dynamic instability [3, 4] is now accepted as the dominant mechanism governing the dynamics of microtubule polymerization. Each polymerizing microtubule persistently grows for a prolonged duration and, then makes a sudden transition to a depolymerizing phase; this phenomenon is known as “catastrophe”. However, the rapid shrinking of a depolymerizing microtubule can get arrested when it makes a sudden reverse transition, called “rescue”, to a polymerizing phase. It is now generally believed that the dynamic instability of a microtubule is triggered by the loss of its *guanosine triphosphate* (GTP) cap because of the hydrolysis of GTP into guanosine diphosphate (GDP). But, the detailed mechanism, i.e., how the chemical process of cap loss induces mechanical instability, remains far from clear.

The dynamics of polymerization-depolymerization of microtubules and the phenomena of “catastrophe” and “rescue” [5, 6, 7, 8], have been studied extensively over the last decade using simple theoretical models [9, 10, 11, 12, 13, 14, 15, 16, 17, 18, 19, 20, 21]. One of the earliest models of polymerization-depolymerization dynamics of microtubules was proposed by Hill [9] and subsequently extended by Rubin and coworkers [10, 19]. The length of the microtubules is *discrete* in the Hill model which is formulated in terms of two infinite sets of coupled ordinary differential equations. Dogterom and Leibler [11, 12], however, treated the length as a *continuous* variable and the dynamical equations were reduced to just two coupled partial differential equations.

A large number of different types of antimetabolic drug molecules are known to bind with free tubulins in solution and/or with tubulins in microtubules. The polymerization-depolymerization dynamics of microtubules, which play crucial roles in mitosis, is strongly influenced by these drugs. The effects of various drug molecules, e.g., *colchicine*, paclitaxel, vinca alkaloids and *taxol*, etc., on the dynamics of microtubules have been investigated experimentally for several years [22, 23, 24], partly because of their potential clinical use in combating cancer [25, 26, 27]. These drugs can be broadly classified into two groups. One group consists of microtubule-destabilizing agents whereas the members of the other group are microtubule-stabilizing agents.

In this paper we are interested in the effects of microtubule-stabilizing agents (i.e., catastrophe-suppressing drugs) on the length distributions of the microtubules in the absence of any GTP and GDP in the system. The drug molecules of our interest, e.g., *vinblastine*, bind rapidly with free tubulins in solution; when such a tubulin-drug complex binds with the growing end of a microtubule, the drug-capped microtubule gets stabilized because of the strong suppression of catastrophe phenomenon [26, 27].

The aim of this paper is to investigate *theoretically*

*Corresponding author

†Electronic address: debch@iitk.ac.in

the generic effects of *catastrophe-suppressing* drugs by extending the earlier theoretical models, developed by Hill [9] and Freed [20], for the dynamics of polymerization of drug-free pure tubulins. We derive exact analytical expressions for the steady-state distributions of the lengths of the microtubules tipped with the drug-bound tubulin subunits as well as those of microtubules tipped with pure (i.e., drug-free) tubulin subunits. We carry out linear stability analysis of the steady-state distributions and physically interpret the implications of the spectrum of the eigenvalues of the stability matrix.

This paper is organized as follows. In section II we briefly review some of the relevant earlier theoretical models of dynamic instability. In particular, we summarize the mathematical frameworks of the Hill model [9] and the recent Freed model [20] of dynamic instability of microtubules. In section III we propose an extension of the Hill model so as to capture the effects of the catastrophe-suppressing drugs in a simple way. The model is made more realistic in section IV by treating the dynamics of the concentration of the drug-free tubulins explicitly following a Freed-like approach. The paper ends with a conclusion section V.

II. BRIEF REVIEW OF EARLIER MODELS OF DYNAMIC INSTABILITY

A. Hill model

Microtubules consist of 13 protofilaments, each consisting of monomeric units (actually a $\alpha - \beta$ heterodimer) each of which is approximately 8 nm long. On the other hand, the polymers in the Hill model are one-dimensional. Therefore, some authors (see, for example, [28]) identify “monomeric units” of the one-dimensional Hill model to have a length of approximately $8/13 = 0.6$ nm.

Let $P_H^+(n, t)$ and $P_H^-(n, t)$ be the probabilities of finding a microtubule of length n , at time t , in the growing (+) and shrinking (−) phases, respectively. Moreover, let $P_H(0, t)$ be the probability that the MT nucleating site is empty at time t . Furthermore, we denote the growth rate of the growing microtubules and decay rate of the shrinking microtubules by p_g^H and p_d^H , respectively, while the frequencies of catastrophes (the transition from growing to the shrinking phase) and rescues (the transition from the shrinking to growing phase) are denoted by the symbols p_{+-}^H and p_{-+}^H , respectively. Interestingly, the four parameters p_g^H , p_d^H , p_{+-}^H and p_{-+}^H were measured as functions of free tubulin concentration first in 1988 [29] by observing single microtubules using video light microscopy. However, the concentration dependence of these parameters, if any, does not appear explicitly in the Hill model.

The Master equations for these probabilities are given

by [9]

$$\frac{dP_H^+(n, t)}{dt} = p_g^H P_H^+(n-1, t) + p_{-+}^H P_H^-(n, t) - (p_g^H + p_{+-}^H) P_H^+(n, t), \text{ for } n \geq 2, \quad (1)$$

$$\frac{dP_H^-(n, t)}{dt} = p_d^H P_H^-(n+1, t) + p_{+-}^H P_H^+(n, t) - (p_d^H + p_{-+}^H) P_H^-(n, t), \text{ for } n \geq 1, \quad (2)$$

$$\frac{dP_H^+(1, t)}{dt} = p_g^H P_H(0, t) + p_{-+}^H P_H^-(1, t) - (p_g^H + p_{+-}^H) P_H^+(1, t), \quad (3)$$

and

$$\frac{dP_H(0, t)}{dt} = -p_g^H P_H(0, t) + p_d^H P_H^-(1, t). \quad (4)$$

Imposing the normalization

$$\sum_{n=1}^{\infty} P_H^+(n) + \sum_{n=1}^{\infty} P_H^-(n) + P_H(0) = 1, \quad (5)$$

the steady-state solutions of the equations (1)-(4) are given by [9]

$$P_H^+(n) = x_H^n P_H(0), \quad (6)$$

and

$$P_H^-(n) = x_H^{n-1} y_H P_H(0) \quad (7)$$

with

$$P_H(0) = \frac{1 - x_H}{1 + y_H}, \quad (8)$$

$$x_H = \frac{p_g^H (p_d^H + p_{-+}^H)}{p_d^H (p_g^H + p_{+-}^H)} \quad (9)$$

and

$$y_H = \frac{p_{+-}^H}{p_d^H}. \quad (10)$$

In order that the distributions $P_H^\pm(n)$ are decreasing, rather than increasing, functions of n we must have $x_H < 1$ which imposes the constraint $p_g^H (p_d^H + p_{-+}^H) < p_d^H (p_g^H + p_{+-}^H)$, i.e.,

$$p_g^H p_{-+}^H < p_d^H p_{+-}^H \quad (11)$$

on the magnitudes of the parameters. Interestingly, in the Dogterom-Leibler model [11], a steady-state characterized by exponentially decaying distributions P^\pm of the lengths of the microtubules is attained only if the condition (11) is satisfied by the parameters; otherwise, the system never reaches any steady-state and mean of the (Gaussian) distribution of the lengths of the microtubules continues to increase linearly with time.

B. Freed model

It has been realized for quite some time [16, 17, 29] that the rate of growth of the growing microtubules should depend on the availability of free tubulin monomers in the solution. However, in the Hill model [9] the kinetic rate equations do not involve the concentration of the tubulin monomers. Recently, Freed [20] has generalized the Hill model to incorporate the dependence of the rates on the tubulin monomer concentration. Hammele and Zimmermann [21] carried out independent analytical calculations of the same phenomenon by extending the Dogterom-Leibler [11] model. Since our calculations in the section IV are based on an extension of Freed's model, we summarize here the main points of this approach.

Suppose, ρ_0 is the initial concentration of the tubulin subunits and ρ is the corresponding instantaneous concentration at time t . Similarly, N_0 and N are the initial and instantaneous concentrations of the free (i.e., without bound tubulin) nucleating sites, respectively. The symbols $P_F^\pm(n, t)$ in this section denote the *concentrations*, rather than probabilities, of microtubules in the growing and the shrinking phases, respectively. Moreover, binding of a tubulin subunit with a free nucleating site takes place at a rate p_n^F . Using these quantities, the kinetic rate equations in the Freed model [20] can now be written as

$$\frac{dP_F^+(n, t)}{dt} = p_g^F \rho P_F^+(n-1, t) + p_{-+}^F P_F^-(n, t) - (p_g^F \rho + p_{+-}^F) P_F^+(n, t), \text{ for } n \geq 2, \quad (12)$$

$$\frac{dP_F^-(n, t)}{dt} = p_d^F P_F^-(n+1, t) + p_{+-}^F P_F^+(n, t) - (p_d^F + p_{-+}^F) P_F^-(n, t), \text{ for } n \geq 1, \quad (13)$$

$$\frac{dP_F^+(1, t)}{dt} = p_n^F \rho N + p_{-+}^F P_F^-(1, t) - (p_g^F \rho + p_{+-}^F) P_F^+(1, t), \quad (14)$$

and

$$\frac{d\rho}{dt} = -p_n^F \rho N - p_g^F \rho \sum_{n=1}^{\infty} P_F^+(n, t) + p_d^F \sum_{n=1}^{\infty} P_F^-(n, t). \quad (15)$$

Moreover, tubulin mass conservation imposes the condition

$$\rho_0 = \rho + Q_F^+ + Q_F^- \quad (16)$$

where

$$Q_F^\pm = \sum_{n=1}^{\infty} n P_F^\pm(n, t). \quad (17)$$

Furthermore,

$$N_0 = N + P_F^+ + P_F^- \quad (18)$$

where

$$P_F^\pm = \sum_{n=1}^{\infty} P_F^\pm(n, t). \quad (19)$$

There is one-to-one correspondence between the parameters and dynamical variables in the Freed model and those in the Hill model. For example, $p_g^F \rho, p_d^F, p_{+-}^F$ and p_{-+}^F correspond to p_g^H, p_d^H, p_{+-}^H and p_{-+}^H , respectively.

The steady-state solution of this system of kinetic equations is given by [30]

$$P_F^+ = p_n^F N_0 \rho (p_{-+}^F + p_d^F) / D \quad (20)$$

$$P_F^- = p_n^F N_0 \rho (p_{+-}^F + p_g^F \rho) / D \quad (21)$$

and

$$P_F^-(1) = \beta' = p_n^F N_0 \rho (p_d^F p_{+-}^F - p_g^F \rho p_{-+}^F) / (p_d^F D) \quad (22)$$

where

$$D = p_n^F p_g^F \rho^2 + (p_d^F p_n^F + p_n^F p_{+-}^F - p_g^F p_{-+}^F) \rho + (p_d^F p_{+-}^F + p_n^F \rho p_{-+}^F). \quad (23)$$

Finally, using a generating function technique, Freed[20] derived the analytical expressions

$$P_F^+(n) = (a' c')^{(n-1)/2} [(f' + \beta' d') U_{n-1}(\lambda') - (a' c')^{-1/2} a' f' U_{n-2}(\lambda')] \quad (24)$$

and

$$P_F^-(n) = (a' c')^{(n-1)/2} [\beta' U_{n-1}(\lambda') + (a' c')^{-1/2} (b' f' - c' \beta') U_{n-2}(\lambda')] \text{ for } n \geq 2, \quad (25)$$

where

$$a' = (p_d^F + p_{-+}^F) / p_d^F, \quad (26)$$

$$b' = -p_{+-}^F / p_d^F, \quad (27)$$

$$c' = p_g^F \rho / (p_g^F \rho + p_{+-}^F), \quad (28)$$

$$d' = p_{-+}^F / (p_g^F \rho + p_{+-}^F), \quad (29)$$

$$f' = p_n^F \rho N / (p_g^F \rho + p_{+-}^F). \quad (30)$$

$$\lambda' = (a' + b' d' + c') / [2(a' c')^{1/2}] \quad (31)$$

and $U_n(\lambda')$ are the Chebyshev polynomial of the second kind given by

$$U_n(\lambda') = \sin[(n+1) \arccos \lambda'] / (1 - \lambda'^2)^{1/2}, \quad (32)$$

together with $U_{-1}(\lambda') = 0$.

The distributions $P_F^\pm(n)$ will be decreasing functions of n provided the condition $a'c' < 1$ is satisfied; this condition imposes the constraint

$$p_g^F \rho p_{-+}^F < p_d^F p_{+-}^F \quad (33)$$

on the magnitudes of the parameters and the value of the drug-free tubulin subunits ρ in the steady-state. The condition (33) becomes identical to (11) if we identify $p_g^F \rho$ with p_g^H .

While expressing the steady-state distributions $P_F^\pm(n)$ in terms of Chebyshev polynomial, Freed [20] implicitly assumed that $|\lambda'| < 1$. However, as shown in appendix A, λ' is, in general, larger than unity. We revise the Freed's result in section IV by taking $\lambda' \geq 1$ and, consequently, we get a different polynomial instead of the Chebyshev polynomial given in (32).

Freed [20] derived the exact form of the stability ma-

trix. we define

$$\Delta_\pm = \sum_{n=1}^{\infty} \delta P_\pm(n) \quad (34)$$

and the column vectors

$$\mathbf{V}(t) = \begin{pmatrix} \Delta_+ \\ \Delta_- \\ \delta \rho \end{pmatrix} \quad (35)$$

$$\mathbf{N}_F = \begin{pmatrix} 0 \\ -p_d \\ 0 \end{pmatrix} \quad (36)$$

The, the equations obtained from the linear stability analysis above can be written as

$$\frac{d\mathbf{V}(t)}{dt} = \mathbf{M}_F \mathbf{V}(t) + \mathbf{N}_F \delta P_-^F(1) \quad (37)$$

where the matrix \mathbf{M}_F is given by

$$\mathbf{M}_F = \begin{pmatrix} -p_{+-} - p_n[\rho]_{ss} & p_{-+} - p_n[\rho]_{ss} & \mathbf{M}_{13} \\ p_{+-} & -p_{-+} & 0 \\ (p_n - p_g)[\rho]_{ss} & p_n[\rho]_{ss} + p_d & \mathbf{M}_{33} \end{pmatrix} \quad (38)$$

with

$$\mathbf{M}_{13} = p_n \{N_0 - [P_+]_{ss} - [P_-]_{ss}\} \quad (39)$$

and

$$\mathbf{M}_{33} = (p_n - p_g)[P_+]_{ss} - p_n(N_0 - [P_-]_{ss}) \quad (40)$$

The nature of the stability of the steady-state is determined by the eigenvalues of the matrix \mathbf{M}_F . The steady state is stable if all the eigenvalues are real and negative. On the other hand, if some roots are positive, these would indicate unbounded growth and the corresponding steady-state would be unstable. If the characteristic equation has a pair of complex conjugate roots then the system will either oscillate about the steady state (if the real part is negative) or exhibit oscillatory unbounded growth (if the real part is positive).

We have carried out numerical analysis of this stability matrix and obtained the eigenvalues for several sets of values of the model parameters; the eigenvalues corresponding to five different values of ρ , for a fixed set of values of the other model parameters, are shown in the table I. Thus, the steady-state distribution is stable over the entire range of ρ for the chosen set of parameters values.

ρ	m_1	m_2	m_3
0.4	-49.984	-0.282	-23.719
0.8	-99.999	-0.295	-22.507
1.6	-199.999	-0.299	-20.456
2.0	-250.000	-0.299	-19.566
2.5	-312.500	-0.300	-18.577

TABLE I: The eigenvalues of the linear stability matrix \mathbf{M}_F in the Freed model. The other common parameters for above table are $p_g = 125, p_d = 900, p_{-+} = 0.08, p_{+-} = 0.22, N_0 = 0.2$ (in respective units).

III. HILL-LIKE MODEL WITH DRUGS

Let p_c^h be the rate of growth of a microtubule by addition of a drug-bound tubulin. Since addition of catastrophe-suppressing drugs to the system strongly reduce the catastrophe frequency, *we assume that the drug is such that it arrests catastrophe. In other words, a microtubule tipped with a drug-bound tubulin can grow but cannot shrink.* We shall use the symbol $\Pi_h(n, t)$ to denote the probability of a microtubule, tipped with a drug-bound tubulin, that has length n at time t . As a consequence of our assumption, we do not need to con-

sider the two quantities $\Pi_h^+(n, t)$ and $\Pi_h^-(n, t)$ separately; $\Pi_h^-(n, t) = 0$ for all n at all t . However, even in the presence of such drugs in the system, catastrophes can take place in microtubules tipped with drug-free tubulins. The distributions of the microtubules tipped with drug-free tubulin subunits in the growing and shrinking phases are denoted by $P_h^+(n, t)$ $P_h^-(n, t)$, respectively.

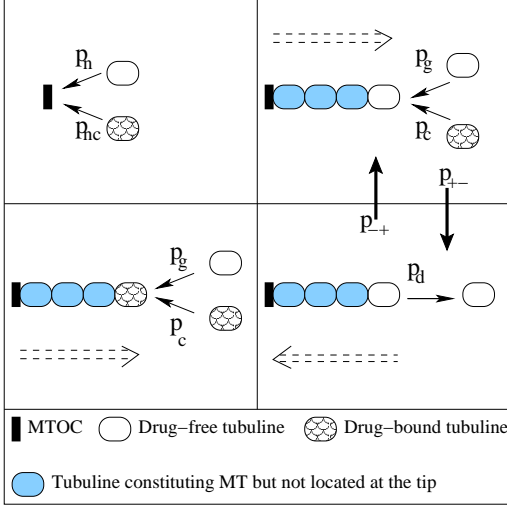


FIG. 1: A schematic description of our Hill-like model in the presence of catastrophe-suppressing drugs. The superscript h has been dropped from the symbols denoting the model parameters.

Thus, the equations (1)-(4) are generalized to the forms

$$\begin{aligned} \frac{dP_h^+(n, t)}{dt} &= p_g^h [P_h^+(n-1, t) + \Pi_h(n-1, t)] + p_{-+}^h P_h^-(n, t) \\ &\quad - (p_g^h + p_c^h + p_{+-}^h) P_h^+(n, t), \text{ for } n \geq 2, \end{aligned}$$

$$\begin{aligned} \frac{dP_h^-(n, t)}{dt} &= p_d^h P_h^-(n+1, t) + p_{+-}^h P_h^+(n, t) \\ &\quad - (p_d^h + p_{-+}^h) P_h^-(n, t), \text{ for } n \geq 1, \end{aligned} \quad (42)$$

$$\frac{dP_h^+(1, t)}{dt} = p_g^h P_h(0, t) + p_{-+}^h P_h^-(1, t) - (p_g^h + p_c^h + p_{+-}^h) P_h^+(1, t), \quad (43)$$

$$\frac{dP_h(0, t)}{dt} = -(p_g^h + p_c^h) P_h(0, t) + p_d^h P_h^-(1, t), \quad (44)$$

$$\begin{aligned} \frac{d\Pi_h(n, t)}{dt} &= p_c^h [\Pi_h(n-1, t) + P_h^+(n-1, t)] \\ &\quad - (p_g^h + p_c^h) \Pi_h(n, t), \text{ for } n \geq 2, \end{aligned} \quad (45)$$

$$\frac{d\Pi_h(1, t)}{dt} = p_c^h P_h(0, t) - (p_g^h + p_c^h) \Pi_h(1, t). \quad (46)$$

In order to distinguish between the Hill model and our Hill-like model with catastrophe-suppressing drugs, we replace the subscripts (and superscripts) H of the former by h in the latter.

The steady-state solutions of these kinetic equations (see appendix B for details) are

$$P_h^+(n) = x_h (x_h + z_h)^{n-1} P_h(0), \quad (47)$$

$$P_h^-(n) = y_h (x_h + z_h)^{n-1} P_h(0), \quad (48)$$

$$\Pi_h(n) = z_h (x_h + z_h)^{n-1} P_h(0), \quad (49)$$

where

$$P_h(0) = \frac{1 - x_h - z_h}{1 + y_h} \quad (50)$$

with

$$x_h = \frac{p_g^h (p_d^h + p_{-+}^h) + p_c^h p_{-+}^h}{p_d^h (p_g^h + p_{+-}^h) + p_c^h p_d^h} \quad (51)$$

and

$$y_h = \frac{p_g^h + p_c^h}{p_d^h} \quad (52)$$

$$z_h = \frac{p_c^h}{p_c^h + p_g^h} \quad (53)$$

The distributions (51-53) are decreasing functions of n (41) provided $(x_h + z_h) < 1$, i.e.,

$$(p_g^h + p_c^h)^2 p_{-+}^h < p_g^h p_d^h p_{+-}^h \quad (54)$$

this condition (54) reduces to the condition (11) in the limit $p_c^h \rightarrow 0$. Note that in the limit $p_c^h \rightarrow 0$, $z_h \rightarrow 0$ while the expressions (51) and (52) for x_h and y_h reduce to x_H and y_H given by the expressions (9) and (10), respectively; hence, in this limit, $\Pi_h(n) \rightarrow 0$ and the expressions (47) and (48) for $P_h^\pm(n)$ reduce to the corresponding expressions (6) and (7) for $P_H^\pm(n)$.

The parameters $p_g^h, p_d^h, p_{+-}^h, p_{-+}^h$, etc. have dimensions [$time^{-1}$]. For a typical set of values of these parameters, we have plotted the distributions $P_h^+(n)$, $P_h^-(n)$ and $\Pi_h(n)$ in fig.2(a),(b) and (c), respectively, each for several different numerical values of p_c^h . The straight lines on the semi-log plots is a reflection of the exponential decay of the distribution with increasing length of the microtubules. Moreover, the longer tails of these distributions at higher values of p_c^h demonstrates that higher p_c^h causes stronger suppression of the *catastrophe* phenomenon.

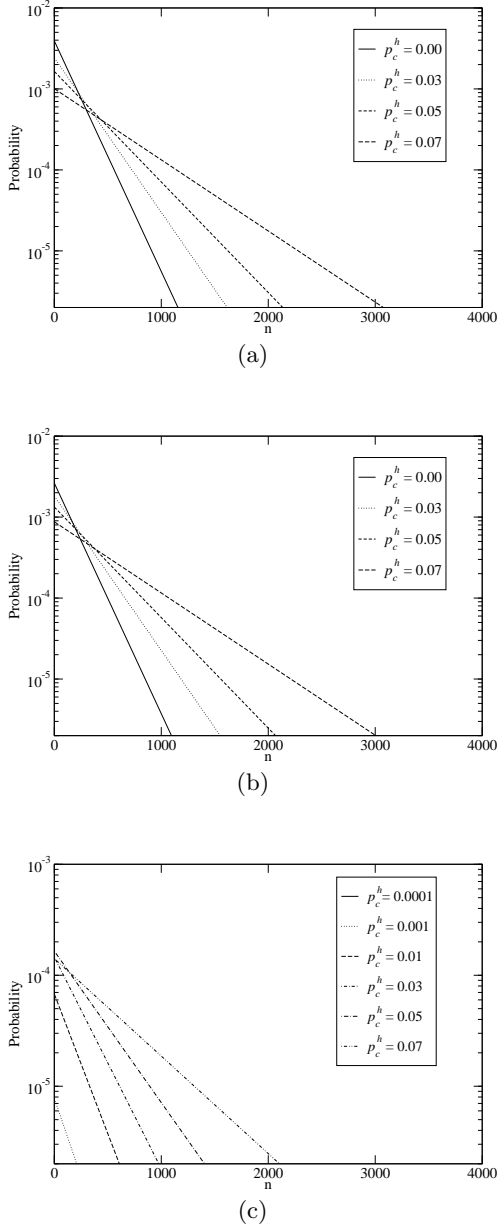


FIG. 2: The steady-state distributions (a) $P_h^+(n)$, (b) $P_h^-(n)$ and (c) $\Pi_h(n)$ of the size n of microtubules in our Hill-like model in the presence of catastrophe-suppressing drugs are plotted for several values of p_c^h ; the common parameters are $p_g^h = 0.5$, $p_d^h = 0.75$, $p_{+-}^h = 0.01$ and $p_{-+}^h = 0.01$, each *per unit time*.

A. Stability of the steady-state

Let us define the small deviations

$$\delta P_h^\pm(n) = P_h^\pm(n, t) - [P_h^\pm]_{ss} \quad (55)$$

$$\delta \Pi_h(n) = \Pi_h(n, t) - [\Pi_h]_{ss} \quad (56)$$

from the corresponding steady-states where the steady-state values $[P_\pm]_{ss}$ and $[\Pi]_{ss}$ are given by the equations

(47), (48) and (49), respectively. Linear stability analysis of the steady-state distributions leads to the equations

$$\begin{aligned} \frac{d\delta P_h^+(n, t)}{dt} &= p_g^h [\delta P_h^+(n-1, t) + \delta \Pi_h(n-1, t)] \\ &\quad + (p_g^h + p_c^h + p_{+-}^h) \delta P_h^+(n, t) \quad \text{for } n \geq 2 \end{aligned} \quad (57)$$

$$\begin{aligned} \frac{d\delta P_h^-(n, t)}{dt} &= p_d^h \delta P_h^-(n+1, t) + p_{+-}^h \delta P_h^+(n, t) \\ &\quad - (p_d^h + p_{-+}^h) \delta P_h^-(n, t) \\ &\quad \text{for } n \geq 1 \end{aligned} \quad (58)$$

$$\begin{aligned} \frac{d\delta \Pi_h(n, t)}{dt} &= p_c^h \{ \delta \Pi_h(n-1, t) + \delta P_h^+(n-1, t) \} \\ &\quad - (p_g^h + p_c^h) \delta \Pi_h(n, t) \quad \text{for } n \geq 2 \end{aligned} \quad (59)$$

$$\begin{aligned} \frac{d\delta P_h^+(1, t)}{dt} &= p_g^h \delta P(0, t) + p_{-+}^h \delta P_h^-(1, t) \\ &\quad - (p_g^h + p_c^h + p_{+-}^h) \delta P_h^+(1, t) \end{aligned} \quad (60)$$

$$\frac{d\delta \Pi_h(1, t)}{dt} = p_c^h \delta P(0, t) - (p_g^h + p_c^h) \delta \Pi_h(1, t) \quad (61)$$

Using the normalization condition we get

$$\delta P(0, t) = - \sum_{n=1}^{\infty} \delta P_h^+(n, t) - \sum_{n=1}^{\infty} \delta P_h^-(n, t) - \sum_{n=1}^{\infty} \delta \Pi_h(n, t) \quad (62)$$

Next, we define

$$\Delta_\pm = \sum_{n=1}^{\infty} \delta P_h^\pm(n) \quad (63)$$

$$\Delta_0 = \sum_{n=1}^{\infty} \delta \Pi_h(n) \quad (64)$$

and the column vectors

$$\mathbf{W}(t) = \begin{pmatrix} \Delta_+ \\ \Delta_- \\ \Delta_0 \end{pmatrix} \quad (65)$$

$$\mathbf{N}_h = \begin{pmatrix} 0 \\ -p_d^h \\ 0 \end{pmatrix} \quad (66)$$

The equations obtained from the linear stability analysis above can be written as

$$\frac{d\mathbf{W}(t)}{dt} = \mathbf{M}_h \mathbf{W}(t) + \mathbf{N}_h \delta P_h^-(1, t) \quad (67)$$

where the matrix \mathbf{M}_h is given by

$$\mathbf{M}_h = \begin{pmatrix} -(p_c^h + p_{+-}^h - p_g^h) & p_{-+}^h - p_g^h & 0 \\ p_{+-}^h & -p_{-+}^h & 0 \\ 0 & -p_c & -(p_g^h + p_c^h) \end{pmatrix} \quad (68)$$

p_c^h	m_1	m_2	m_3
0	-100.000	-100.000	-0.300
10	-100.020	-100.000	-0.280
20	-120.037	-120.000	-0.263
30	-130.051	-130.000	-0.249
50	-150.073	-150.000	-0.227
100	-200.110	-200.000	-0.190
150	-250.132	-250.000	-0.168

TABLE II: The eigenvalues of the linear stability matrix \mathbf{M}_h in our Hill-like model. The common parameters are $p_g^h = 100$, $p_d^h = 900$, $p_{-+}^h = 0.08$, $p_{+-}^h = 0.22$, (each per *unit time*)

Note that all the eigenvalues remain negative up to a reasonably high value of p_c corresponding to the parameter set chosen for the table II. This result indicates that the steady state distributions of the lengths of the microtubules, which we have derived in this section, remain stable up to a moderately high dosage of the catastrophe suppressing drug.

IV. EFFECTS OF DRUGS ON MT: A HYBRID HILL-FREED-LIKE MODEL

In this section we extend the Hill-like model developed in section III by taking into account the dependence of the rate of growth of the microtubules on the concentration of the drug-free tubulin subunits in the solution; for this purpose we follow the corresponding approach developed by Freed (and reviewed in section II) for microtubule dynamics in the absence of drugs. However, the effects of the drug-bound tubulin subunits are taken into account in the same way as was done in the Hill-like model presented in the section III. Therefore, the model presented in this section is a *hybrid of Hill-like and Freed-like approaches*; the drug-free tubulins are treated following Freed while the drug-bound tubulins are treated following Hill.

The binding of a drug-bound tubulin subunit with a free nucleating site takes place with probability p_{nc} per unit time. Following Freed, the *concentration* of microtubules of length n which are tipped with drug-bound tubulin subunits is denoted by the symbol $\Pi(n, t)$ while that of the microtubules tipped with drug-free tubulin subunits and in the growing (shrinking) phase is denoted by $P_+(n, t)$ ($P_-(n, t)$). Moreover, all the parameters with identical subscripts in this model and in the Freed model have the same physical significance. The equations of our

interest are

$$\frac{dP_+(n, t)}{dt} = p_g \rho [P_+(n-1, t) + \Pi(n-1, t)] + p_{-+} P_-(n, t) - (p_g \rho + p_c + p_{+-}) P_+(n, t) \quad \text{for } n \geq 2 \quad (69)$$

$$\frac{dP_-(n, t)}{dt} = p_d P_-(n+1, t) + p_{+-} P_+(n, t) - (p_d + p_{-+}) P_-(n, t) \quad \text{for } n \geq 1, \quad (70)$$

$$\frac{d\Pi(n, t)}{dt} = p_c [\Pi(n-1, t) + P_+(n-1, t)] - (p_g \rho + p_c) \Pi(n, t) \quad \text{for } n \geq 2, \quad (71)$$

$$\frac{dP_+(1, t)}{dt} = p_n \rho N + p_{-+} P_-(1, t) - (p_g \rho + p_c + p_{+-}) P_+(1, t), \quad (72)$$

$$\frac{d\Pi(1, t)}{dt} = p_{nc} N - (p_g \rho + p_c) \Pi(1, t), \quad (73)$$

and

$$\frac{d\rho}{dt} = -p_n \rho N - p_g \rho \sum_{n=1}^{\infty} [P_+(n, t) + \Pi(n, t)] + p_d \sum_{n=1}^{\infty} P_-(n, t). \quad (74)$$

The steady state equations are

$$p_n \rho (N_0 - P_+ - P_- - \Pi) = -p_g \rho (P_+ + \Pi) + p_d P_-, \quad (75)$$

$$P_+(n) = c P_+(n-1) + d P_-(n) + c \Pi(n-1), \quad (76)$$

$$P_-(n) = a P_-(n-1) + b P_+(n-1), \quad (77)$$

$$\Pi(n) = e \Pi(n-1) + e P_+(n-1), \quad (78)$$

$$P_+(1) = d P_-(1) + f, \quad (79)$$

$$\Pi(1) = g, \quad (80)$$

where

$$a = (p_d + p_{-+})/p_d, \quad (81)$$

$$b = -p_{+-}/p_d, \quad (82)$$

$$c = p_g \rho / (p_g \rho + p_c + p_{+-}), \quad (83)$$

$$d = p_{-+} / (p_g \rho + p_c + p_{+-}), \quad (84)$$

$$e = p_c / (p_g \rho + p_c), \quad (85)$$

$$f = p_n \rho N / (p_g \rho + p_c + p_{+-}), \quad (86)$$

and

$$g = p_{nc} N / (p_g \rho + p_c). \quad (87)$$

Note that in the limit of vanishing concentration of drug-bound tubulin, i.e., $p_c \rightarrow 0$, the expressions (81)- (84) for a, b, c , and d reduce to the expressions (26)-(29) for a', b', c' and d' , respectively. Moreover, in the limit $p_c \rightarrow 0$ and $p_{nc} \rightarrow 0$, equations (85) and (87) imply $e \rightarrow 0$ and $g \rightarrow 0$ while the expression (86) reduces to the corresponding expression (30) of the original Freed model.

Defining

$$\begin{aligned} P_+ &= \sum_{n=1}^{\infty} P_+(n), \\ P_- &= \sum_{n=1}^{\infty} P_-(n), \\ \Pi &= \sum_{n=1}^{\infty} \Pi(n), \end{aligned} \quad (88)$$

we obtain the following three equations from (77), (76) and (78),

$$(1 - a)P_- - bP_+ = P_-(1), \quad (89)$$

$$(1 - c)P_+ - c\Pi - dP_- = f, \quad (90)$$

$$(1 - e)\Pi - eP_+ = \Pi(1), \quad (91)$$

We solve for P_+ , P_- and Π using (90), (91) and (75). Substituting these solutions in (89), we obtain $P_-(1)$ at the steady state. Finally, steady state expressions for $P_+(1)$ and $\Pi(1)$ are obtained from (79) and (80).

The solutions of linear equations (90), (91) and (75) can be obtained in a straightforward way. The solutions are

$$P_+ = \frac{\rho N_0 p_g p_2 (\rho p_n + p_{nc})}{\mathcal{D}}, \quad (92)$$

$$P_- = \frac{\rho N_0 p_g (\rho p_n + p_{nc}) (p_1 + \rho p_g)}{\mathcal{D}}, \quad (93)$$

$$\Pi = \frac{N_0 [\rho p_c p_n p_2 - \rho p_g p_{-+} p_{nc} + p_d p_{nc} p_1]}{\mathcal{D}}, \quad (94)$$

$$P_-(1) = \frac{\rho N_0 p_g (\rho p_n + p_{nc}) (p_{+-} p_d - p_c p_{-+} - \rho p_{-+} p_g)}{(p_d \mathcal{D})}, \quad (95)$$

where

$$\begin{aligned} \mathcal{D} &= \rho^3 p_g^2 p_n + p_d p_{nc} p_1 + \rho^2 p_g^2 (p_{nc} - p_{-+}) \\ &+ \rho^2 p_g p_n (p_1 + p_2) + \rho p_c p_2 p_n + \rho p_g p_c (p_{nc} - p_{-+}) \\ &+ \rho p_g p_{nc} p_{+-} + \rho p_g p_d (p_{nc} + p_{+-}), \end{aligned} \quad (96)$$

with

$$p_1 = p_c + p_{+-} \quad (97)$$

and

$$p_2 = p_d + p_{-+}. \quad (98)$$

In the following the generating function method is used to obtain the $P_+(n)$, $P_-(n)$ and $\Pi(n)$ for arbitrary n . We proceed by multiplying both sides of equations (76), (77) and (78) by x^n and then summing over n from $n = 1$ to ∞ . Defining

$$P_+(x) = \sum_{n=1}^{\infty} P_+(n) x^n, \quad (99)$$

$$P_-(x) = \sum_{n=1}^{\infty} P_-(n) x^n \quad (100)$$

and

$$\Pi(x) = \sum_{n=1}^{\infty} \Pi(n) x^n, \quad (101)$$

we have the following equations for $P_+(x)$, $P_-(x)$ and $\Pi(x)$:

$$(1 - cx)P_+(x) - dP_-(x) - cx\Pi(x) = xf \quad (102)$$

$$bxP_+(x) + (ax - 1)P_-(x) = -x\beta \quad (103)$$

$$exP_+(x) + (ex - 1)\Pi(x) = -xg \quad (104)$$

where $\beta = P_-(1)$. Solving this set of linear equations for $P_+(x)$, $P_-(x)$ and $\Pi(x)$, we find

$$P_+(x) = \frac{(aef - acg)x^3 - (\beta de - cg + ef + af)x^2 + (\beta d + f)x}{\Delta}, \quad (105)$$

$$P_-(x) = \frac{(bcg - bef)x^3 + (bf - \beta c - \beta e)x^2 + \beta x}{\Delta}, \quad (106)$$

$$\Pi(x) = \frac{(acg - aef)x^3 + (\beta de - cg + ef - ag - bdg)x^2 + gx}{\Delta}. \quad (107)$$

where

$$\Delta = (ac + ae + bde)x^2 - (a + c + e + bd)x + 1. \quad (108)$$

$$P_+(x) = \frac{(aef - acg)x^3 - (\beta de - cg + ef + af)x^2 + (\beta d + f)x}{y^2 - 2\lambda y + 1}, \quad (109)$$

$$P_-(x) = \frac{(bcg - bef)x^3 + (bf - \beta c - \beta e)x^2 + \beta x}{y^2 - 2\lambda y + 1}, \quad (110)$$

$$\Pi(x) = \frac{(acg - aef)x^3 + (\beta de - cg + ef - ag - bdg)x^2 + gx}{y^2 - 2\lambda y + 1}. \quad (111)$$

where

$$\lambda = (a + e + c + bd)/[2(ac + ae + bde)^{1/2}]. \quad (112)$$

and

$$y = (a + e + c + bd)^{1/2}x. \quad (113)$$

Solutions for $P_{\pm}(n)$ and $\Pi(n)$ can be obtained by expanding term

$$\frac{1}{y^2 - 2\lambda y + 1} \quad (114)$$

in the above equations using Taylor series expansion for $\lambda \geq 1$ and $y < 1$ and then equating the coefficients of y^n on both sides. Thus, the expressions for $P_{\pm}(n)$ and $\Pi(n)$ are as follows:

$$P_+(n) = \alpha^{(n-1)/2}[\alpha_3 U_{n-1}(\lambda) - \alpha_2 U_{n-2}(\lambda) + \alpha_1 U_{n-3}(\lambda)] \quad \text{for } n \geq 2, \quad (115)$$

$$P_+(1) = \alpha_3 U_0(\lambda) \quad (116)$$

where

$$\alpha = (ac + ae + bde), \quad (117)$$

$$\alpha_1 = (aef - acg)/\alpha, \quad (118)$$

$$\alpha_2 = (\beta de - cg + ef + af)/\alpha^{1/2}, \quad (119)$$

$$\alpha_3 = (\beta d + f), \quad (120)$$

$$(121)$$

and

$$U_n(\lambda) = \sum_{m=0}^{[n/2]} (-1)^m \frac{(n-m)!}{m!(n-2m)!} (2\lambda)^{n-2m}, \quad (122)$$

with $U_{-1}(\lambda) = 0$, where the symbol $[n/2]$ represents the largest integer smaller than or equal to $n/2$. Similarly,

$$P_-(n) = \alpha^{(n-1)/2}[\beta U_{n-1}(\lambda) + \beta_2 U_{n-2}(\lambda) + \beta_1 U_{n-3}(\lambda)] \quad \text{for } n \geq 2, \quad (123)$$

$$P_-(1) = \beta U_0(\lambda) \quad (124)$$

where

$$\beta_1 = (bcg - bef)/\alpha \quad (125)$$

$$\beta_2 = (bf - \beta c - \beta e)/\alpha^{1/2}. \quad (126)$$

Finally,

$$\Pi(n) = \alpha^{(n-1)/2}[g U_{n-1}(\lambda) + \gamma_2 U_{n-2}(\lambda) + \gamma_1 U_{n-3}(\lambda)], \quad (127)$$

$$\Pi(1) = g U_0(\lambda) \quad (128)$$

where

$$\gamma_1 = (acg - aef)/\alpha, \quad (129)$$

$$\gamma_2 = (\beta de - cg + ef - ag - bdg)/\alpha^{1/2}. \quad (130)$$

It can be easily checked that these solutions approach Freed's solutions in the limit $p_{nc} \rightarrow 0$, $p_c \rightarrow 0$. In order that the steady state solutions for $P_+(n)$, $P_-(n)$ and $\Pi(n)$ are decreasing, rather than increasing, functions of n , we demand that $\alpha < 1$ which imposes the following constraint on the magnitudes of the parameters:

$$p_{-+}(p_c + \rho p_g)^2 < \rho p_g p_d p_{+-} \quad (131)$$

The condition (131) reduces to the corresponding condition (33) of the Freed model in the limit $p_c \rightarrow 0$.

In order to plot the steady-state distributions (115), (123) and (127) in our hybrid Hill-Freed-like model and to compare these with the distributions (47), (48) and (49) for the same set of parameters, we first converted the concentrations of the different types of microtubules

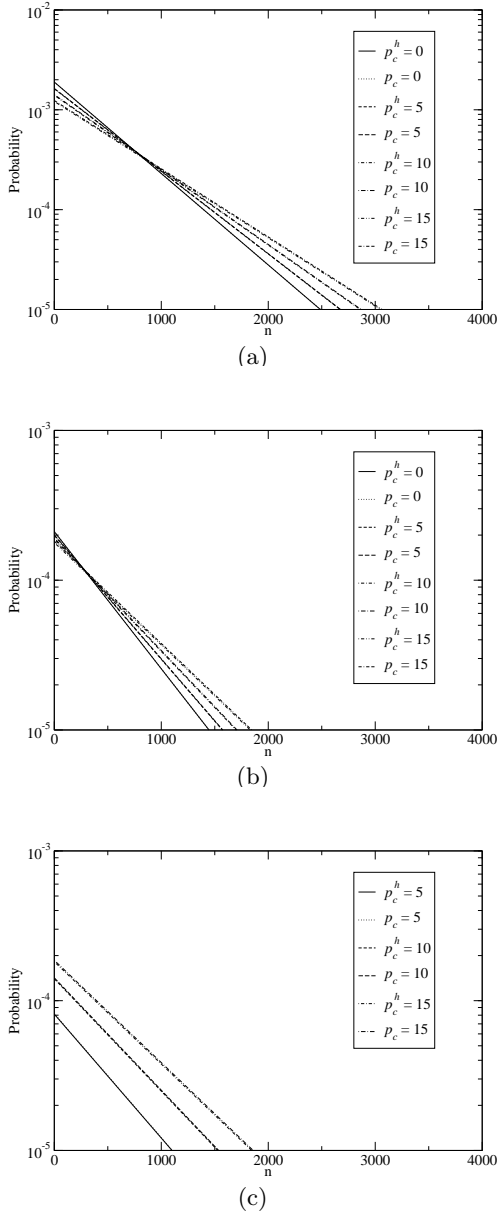


FIG. 3: The steady-state length distributions (a) $P_+(n)$, (b) $P_-(n)$ and (c) $\Pi(n)$ of microtubules in our hybrid model for several values of p_c and compared with corresponding distributions in our Hill-like model (with appropriate rescaling of the parameters and variables following (132)); the common parameters are $p_g = p_n = 125$, $p_d = 900$, $p_{-+} = 0.08$, $p_{+-} = 0.22$, $p_{nc} = p_c$, and $\rho = 0.8$, $N_0 = 0.2$ (in respective units).

of the parameters so as to satisfy the following relations:

$$\begin{aligned} p_g^h &= p_g \rho, \\ p_d^h &= p_d, \\ p_c^h &= p_c, \\ p_{+-}^h &= p_{+-}, \\ p_{-+}^h &= p_{-+}. \end{aligned} \quad (132)$$

The distributions plotted in fig.3 shows that with proper rescaling of the parameters, as mentioned in (132), the results for the Hill-like model and the hybrid Hill-Freed-like model are almost identical. Moreover, the higher is the value of p_c , the longer are the tails of the distributions; this, as explained already in the context of the Hill-like model, is a consequence of the stronger suppression of the catastrophes by higher p_c .

The mean lengths of the microtubules, which correspond to the distributions plotted in the fig.3, are plotted against p_c in fig.4. Surprisingly, for this set of parameter values the mean lengths of the microtubules tipped with drug-bound tubulin and those tipped with drug-free tubulins (both in the growing and shrinking phases) are identical for almost all values of p_c . However, even for this set of parameters values, the fraction of microtubules with drug-bound cap increases with increasing p_c while that with drug-free cap decreases (see fig.5).

We now define the “effective” catastrophe frequency and the “effective” rescue frequency by the relations

$$p_{+-}^{eff} = \frac{p_{+-}P_+}{P_+ + P_- + \Pi} = \frac{p_{+-}P_+}{1 - P_0} \quad (133)$$

and

$$p_{-+}^{eff} = \frac{p_{-+}P_-}{P_+ + P_- + \Pi} = \frac{p_{-+}P_-}{1 - P_0} \quad (134)$$

These “effective” frequencies of catastrophe and rescue are plotted against p_c in fig.6. This trend of variation is qualitatively similar to the corresponding results of laboratory experiments performed with the catastrophe-suppressing drug *vinblastine* [31].

A. Stability of the steady-state

We have obtained the exact analytical expressions for the matrices that decide the stability of the steady-state solutions, which we derived earlier in this section, against small deviations. For this purpose we expand the nonlinear kinetic equations about the steady states and retain only upto the terms linear in the deviations and drop all the terms containing higher orders of deviations.

Let us define the small deviations

$$\delta\rho = \rho(t) - [\rho]_{ss}, \quad (135)$$

into probabilities and, then, chose the numerical values

$$\delta P_{\pm}(n) = P_{\pm}(n, t) - [P_{\pm}]_{ss} \quad (136)$$

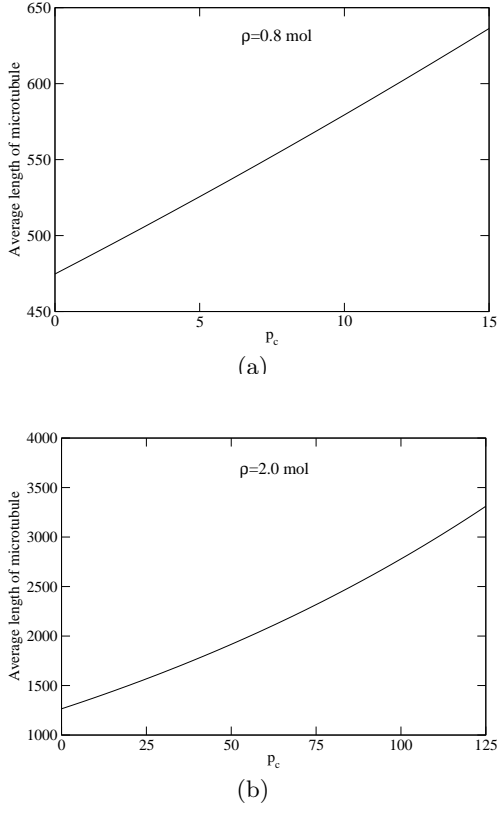


FIG. 4: Mean length of the microtubules in the hybrid model. The numerical values of all the parameters, which are not shown explicitly, are identical to those in fig.3.

$$\delta\Pi(n) = \Pi(n, t) - [\Pi]_{ss} \quad (137)$$

from the corresponding steady-states where the steady-state values $[P_{\pm}]_{ss}$, $[\Pi]_{ss}$, etc. are given by the equations (115), (116), (123), (124), (127), (128), etc. We shall also use the symbols $[P_+]_{ss}$, $[P_-]_{ss}$ and $[\Phi]_{ss}$ to denote the steady-state values of P_+ , P_- and Π given by the equations (88).

Expanding the equations (69)- (74) about the steady state and retaining upto the terms linear in the small deviations we get

$$\begin{aligned} \frac{d\delta P_+(n)}{dt} = & p_g \delta \rho \{ [P_+(n-1)]_{ss} + [\Pi(n-1)]_{ss} \} \\ & + p_g [\rho]_{ss} \{ \delta P_+(n-1) + \delta \Pi(n-1) \} + p_{-+} \delta P_-(n) \\ & - p_g \delta \rho [P_+(n)]_{ss} - p_g [\rho]_{ss} \delta P_+(n) \\ & - (p_c + p_{+-}) \delta P_+(n) \quad \text{for } n \geq 2 \end{aligned} \quad (138)$$

$$\begin{aligned} \frac{d\delta P_-(n)}{dt} = & p_d \delta P_-(n+1) + p_{+-} \delta P_+(n) \\ & - (p_d + p_{-+}) \delta P_-(n) \\ & \text{for } n \geq 1 \end{aligned} \quad (139)$$

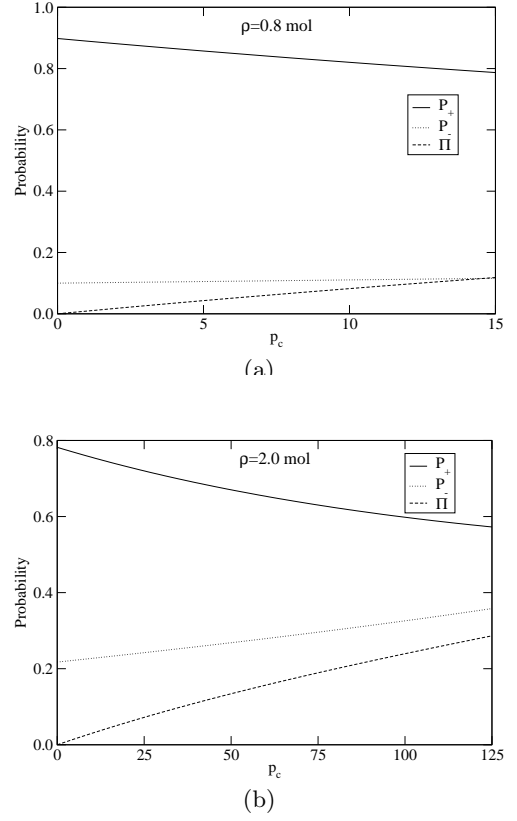


FIG. 5: Fractions of the microtubules that are tipped with drug-free tubulin and are in the growing phase (P_+) or in the shrinking phase (P_-) and those of microtubules tipped with drug-bound tubulin (Π). The numerical values of all the parameters, which are not shown explicitly, are identical to those in the fig.3.

$$\begin{aligned} \frac{d\delta \Pi(n)}{dt} = & p_c \{ \delta \Pi(n-1) + \delta P_+(n-1) \} \\ & - p_g [\rho]_{ss} \delta \Pi(n) - p_g \delta \rho [\Pi(n)]_{ss} - p_c \delta \Pi(n) \\ & \text{for } n \geq 2 \end{aligned} \quad (140)$$

$$\begin{aligned} \frac{d\delta P_+(1)}{dt} = & p_n \tau + p_{-+} \delta P_-(1) \\ & - p_g \{ [\rho]_{ss} \delta P_+(1) + \delta \rho [P_+(1)]_{ss} \} \\ & - (p_c + p_{+-}) \delta P_+(1) \end{aligned} \quad (141)$$

$$\begin{aligned} \frac{d\delta \Pi(1)}{dt} = & p_{nc} \left\{ - \sum_{n=1}^{\infty} \delta P_+(n) - \sum_{n=1}^{\infty} \delta P_-(n) - \sum_{n=1}^{\infty} \delta \Pi(n) \right\} \\ & - p_g \{ [\rho]_{ss} \delta \Pi(1) + \delta \rho [\Pi(1)]_{ss} \} - p_c \delta \Pi(1) \end{aligned} \quad (142)$$

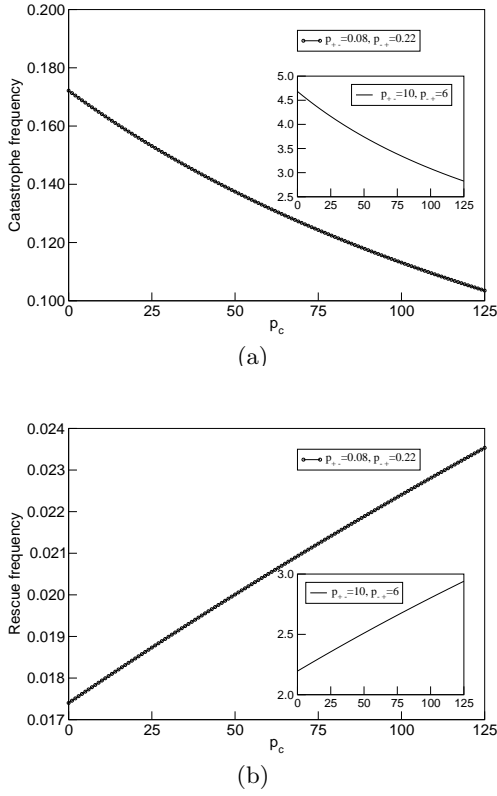


FIG. 6: Effective catastrophe frequency (a) and effective rescue frequency (b), defined through equations (133) and (134), respectively, are plotted against p_c for $\rho = 2.0$. Note the different parameters used for the insets. The numerical values of all the parameters, which are not shown explicitly, are identical to those in the fig.3.

$$\begin{aligned} \frac{d\delta\rho}{dt} = & -p_n\tau - p_g\delta\rho\left\{\sum_{n=1}^{\infty}[P_+(n)]_{ss} + \sum_{n=1}^{\infty}[\Pi(n)]_{ss}\right\} \\ & -p_g[\rho]_{ss}\left\{\sum_{n=1}^{\infty}\delta P_+(n) + \sum_{n=1}^{\infty}\delta\Pi(n)\right\} \\ & +p_d\sum_{n=1}^{\infty}\delta P_-(n) \end{aligned} \quad (143)$$

where

$$\begin{aligned} \tau = & \delta\rho\{N_0 - [\mathcal{P}_+]_{ss} - [\mathcal{P}_-]_{ss} - [\Phi]_{ss}\} \\ & + [\rho]_{ss}\left\{-\sum_{n=1}^{\infty}\delta P_+(n) - \sum_{n=1}^{\infty}\delta P_-(n) - \sum_{n=1}^{\infty}\delta\Pi(n)\right\} \end{aligned} \quad (144)$$

Next, we define

$$\Delta_{\pm} = \sum_{n=1}^{\infty}\delta P_{\pm}(n) \quad (145)$$

$$\Delta_0 = \sum_{n=1}^{\infty}\delta\Pi(n) \quad (146)$$

and the column vectors

$$\mathbf{V}(t) = \begin{pmatrix} \Delta_+ \\ \Delta_- \\ \Delta_0 \\ \delta\rho \end{pmatrix} \quad (147)$$

$$\mathbf{N} = \begin{pmatrix} 0 \\ -p_d \\ 0 \\ 0 \end{pmatrix} \quad (148)$$

The equations obtained from the linear stability analysis above can be written as

$$\frac{d\mathbf{V}(t)}{dt} = \mathbf{M}\mathbf{V}(t) + \mathbf{N}\delta P_-(1) \quad (149)$$

where the matrix \mathbf{M} is given by

$$\mathbf{M} = \begin{pmatrix} -(p_c + p_{+-}) - p_n[\rho]_{ss} & p_{+-} - p_n[\rho]_{ss} & (p_g - p_n)[\rho]_{ss} & \mathbf{M}_{14} \\ p_{+-} & -p_{+-} & 0 & 0 \\ p_c - p_{nc} & -p_{nc} & -p_g[\rho]_{ss} - p_{nc} & -p_g[\Phi]_{ss} \\ (p_n - p_g)[\rho]_{ss} & p_n[\rho]_{ss} + p_d & (p_n - p_g)[\rho]_{ss} & \mathbf{M}_{44} \end{pmatrix} \quad (150)$$

where

$$\mathbf{M}_{14} = p_g[\Phi]_{ss} + p_n\{N_0 - [\mathcal{P}_+]_{ss} - [\mathcal{P}_-]_{ss} - [\Phi]_{ss}\} \quad (151)$$

$$\mathbf{M}_{44} = (p_n - p_g)([\mathcal{P}_+]_{ss} + [\Phi]_{ss}) - p_n(N_0 - [\mathcal{P}_-]_{ss}) \quad (152)$$

The characteristic equation is quartic in the eigenvalue

$\rho = 0.8M$				
p_c	m_1	m_2	m_3	m_4
0	-99.998	-0.295	-22.506	-100.000
5	-105.000	-0.185	-22.633	-104.982
10	-110.000	-0.094	-22.734	-109.972
15	-115.000	-0.019	-22.814	-114.967
16	-116.000	-0.005	-22.828	-115.967
17	-117.000	0.008	-22.842	-116.966
$\rho = 2.0M$				
p_c	m_1	m_2	m_3	m_4
0	-249.999	-0.299	-19.566	-250.000
50	-300.000	-0.121	-19.717	-300.023
100	-350.000	-0.030	-19.785	-350.051
126	-376.000	-0.001	-19.803	-376.061
127	-377.000	0.002	-19.804	-377.062

TABLE III: The eigenvalues of the linear stability matrix \mathbf{M} . The common parameters are $p_g = p_n = 125$, $p_d = 900$, $p_{-+} = 0.08$, $p_{+-} = 0.22$, $p_{nc} = p_c$, $N_0 = 0.2$ (in respective units).

λ . We have systematically investigated the trend of variation of the eigenvalues (m_1, m_2, m_3, m_4) of the matrix \mathbf{M} with the variation of p_c for several sets of values of the other parameters; those for two values of ρ are given in table III. In both these cases, there is a range $0 \leq p_c \leq p_c^{max}$ of values of p_c where all the eigenvalues remain negative indicating stability of the steady state. Moreover, the higher is the steady-state density ρ of the free tubulins in the solution larger is the value of p_c^{max} . As p_c is increased beyond p_c^{max} , one of the negative eigenvalues simply changes sign which indicates instability of the steady-state. The physical reason for the instability of the steady state at sufficiently high p_c is that the higher is the p_c the larger is the fraction of microtubules tipped with drug-bound tubulin which can only grow but cannot shrink.

Thus, although the steady-state distributions of the microtubules in the Hill-like model and those in the hybrid Hill-Freed-like model can be made practically identical by making appropriate correspondence of the parameters in the two models, the latter has a richer dynamics which is reflected also in the linear stability analysis.

V. SUMMARY AND CONCLUSION

In this paper we have developed a model for studying some generic effects of a class of drugs on the polymerization-depolymerization dynamics of microtubules in the absence of GTP and GDP. The class of drugs under consideration suppress catastrophes; one typical example being *vinblastine*. Although there are some superficial similarities between the stabilizing ef-

fect of these drugs in our model and that of the GTP cap in-vivo, there are also crucial differences. A microtubule cannot be in the shrinking phase in our model if it is capped by a drug-bound tubulin just as GTP-capped microtubules are known to remain stable in-vivo. However, a GTP can get hydrolyzed to GDP thereby triggering an instability. In contrast, a catastrophe-suppressing drug molecule in our model does not get hydrolyzed.

One of the two models, namely, the Hill-like model proposed here is an extension of the model developed by Hill [9] to describe microtubule polymerization-depolymerization dynamics in the absence of drugs. Although mathematical treatment of this model is quite simple, it does not take explicitly account for the dynamics of the tubulin concentration in the solution. Therefore, we have also developed a more detailed model in which the effects of the concentration of the pure (i.e., drug-free) tubulin subunits are taken into account in our model in a manner similar to that done by Freed [20] in his recent theoretical study of the microtubule dynamics in the absence of drugs. However, in this model the effects of the tubulin subunits bound to the drug molecules could not be taken into account in a similar manner.

The reason for the difficulty in treating the concentrations of the drug-free and drug-bound tubulins in solution on an equal footing is generic to the Hill-Freed approach. In order that the dynamical equation for the concentration of drug-bound tubulin subunits can reach a steady-state, we have to allow both attachment as well as detachment of the drug-bound subunits to the microtubule. However, if shrinking of a microtubule tipped with drug-bound tubulin is allowed, then, immediately after such a detachment, one needs to know the status of the subunit at the newly exposed tip, i.e., whether the tip consists of a drug-free tubulin or a drug-bound tubulin. But, in the Hill-Freed approach, the system does not have a memory of the past history in the sense that the model does not keep a record of the status (i.e., whether or not bound to a drug molecule) of *all* the tubulin subunits, starting from the nucleation center up to the tip.

Therefore, in order to overcome this technical difficulty, we have incorporated the effects of the drug-bound tubulin subunits in a manner similar to the approach followed in the Hill model [9]. Thus, our second model may be regarded as a hybrid of the Hill-like and Freed-like modeling strategies for the concentrations of the tubulin subunits.

For both the Hill-like model and the Hill-Freed-like hybrid model we have derived exact analytical expressions for the steady-state probability distributions of the lengths of microtubules tipped with drug-bound tubulin subunits as well as those of microtubules tipped with pure (i.e., drug-free) tubulin subunits in the growing and shrinking phases. We have also compared the trends of variations of some of the relevant quantities with the variation of the dosage of the catastrophe-suppressing drug.

We have carried out linear stability analysis of the

steady-states and established that in both the models the length distributions of the microtubules remain stable unless p_c becomes sufficiently high to destabilize the steady-state.

APPENDIX A: ON THE USE OF CHEBYSHEV POLYNOMIAL

It is straight forward to see that

$$\begin{aligned} a' + c' + b'd' &= 1 + \frac{p_g^F \rho(p_d^F + p_{-+}^F)}{p_d^F(p_g^F \rho + p_{+-}^F)} \\ &= 1 + a'c' \end{aligned} \quad (\text{A1})$$

Therefore, re-expressing λ' as

$$\lambda' = \frac{1 + a'c'}{2(a'c')^{1/2}} = \frac{1}{2} \left[\left\{ (a'c')^{1/4} - (a'c')^{-1/4} \right\}^2 + 2 \right] \quad (\text{A2})$$

we find, in general, $\lambda' > 1$.

APPENDIX B: STEADY-STATE SOLUTIONS OF HILL-LIKE MODEL WITH DRUGS

Here we obtain the steady-state solutions of the equations (41)-(46) for Hill-like model in the presence of drugs by equating the RHS of these equations to zero. The solution for $P_-(1)$ is obtained by demanding $dP(0, t)/dt = 0$. This leads to

$$P_-(1) = \frac{(p_g + p_c)}{p_d} P(0) = yP(0) \quad (\text{B1})$$

where y is given by the equation (52). Similarly, claiming $dP_+(1, t)/dt = 0$ and $d\Pi(1, t)/dt = 0$, we have

$$P_+(1) = \frac{[p_g p_d + p_{-+}(p_g + p_c)]}{p_d(p_g + p_c + p_{+-})} P(0) = xP(0) \quad (\text{B2})$$

$$\Pi(1) = \frac{p_c}{p_c + p_g} P(0) = zP(0). \quad (\text{B3})$$

where x and z are given by the equations (51) and (53), respectively. The special case corresponding to $n = 1$ of the equation $dP(n, t)/dt = 0$, leads to the steady state solution for $P_-(2)$,

$$P_-(2) = \frac{1}{p_d} [(p_d + p_{-+})y - p_{+-}x] P(0). \quad (\text{B4})$$

$$(\text{B5})$$

A little bit of algebraic manipulation leads to

$$P_-(2) = y(x + z)P(0). \quad (\text{B6})$$

Steady-state solutions for $P_+(2)$ and $\Pi(2)$ can be obtained in a similar way. Steady-state solutions for $P_-(n)$, $P_+(n)$ and $\Pi(n)$, for arbitrary n , are straightforward generalizations of our observations upto $n = 4$.

Since $P_+(n)$, $P_-(n)$ and $\Pi(n)$ are probabilities of finding microtubules of n subunits in growing, shrinking and in catastrophe-arrested phase, we expect the following normalization condition

$$P(0) + \sum_{n=1}^{\infty} (P_+(n) + P_-(n) + \Pi(n)) = 1. \quad (\text{B7})$$

This leads to the form (50) for $P(0)$.

ACKNOWLEDGMENTS

We thank Balaji Prakash for fruitful discussions and Karl Freed for useful comments on a preliminary draft of the manuscript. DC acknowledges support, in part, from the Deutsche Forschungsgemeinschaft (DFG) through a joint Indo-German joint research project.

-
- [1] B. Alberts, J. Lewis, M. Raff, K. Roberts and J.D. Watson, *Molecular Biology of the Cell* (Garland Publishing, 1994).
 - [2] See the following special issues of journals on the cytoskeleton: V.M. Fowler and R. Vale (eds.) *Curr. Opinion in Cell Biol.* **8**, 1 (1996); B. Geiger and E. Karsenti (eds.) *Curr. Opinion in Cell Biol.* **9**, 1 (1997); Nature Cell Biol. **2**, E1 (1999); M.F. Carrier and G.G. Borisy (eds.) *Curr. Opinion in Cell Biol.* **12**, 17 (2000); D. Nath (ed.) *Nature* 422, 739 (2003).
 - [3] T. Mitchison and M. Kirschner, *Nature* **312**, 232 (1984).
 - [4] T. Mitchison and M. Kirschner, *Nature* **312**, 237 (1984).
 - [5] H. P. Erickson and E.T. O'Brien, *Annu. Rev. Biophys. Biomol. Struct.* **21**, 145 (1992).
 - [6] A. Desai and T. J. Mitchison, *Annu. Rev. Cell Dev. Biol.*, **13**, 83 (1997).

- [7] E. Nogales, *Annu. Rev. Biophys. Biomol. Struct.*, **30**, 397 (2001).
- [8] J. Howard and A. A. Hyman, *Nature*, **422**, 753 (2003).
- [9] T. L. Hill, *Proc. Natl. Acad. Sci.*, **81**, 6728 (1984).
- [10] R. J. Rubin, *Proc. Natl. Acad. Sci.* **85**, 446 (1988).
- [11] M. Dogterom and S. Leibler, *Phys. Rev. Lett.*, **70**, 1347 (1993).
- [12] M. Dogterom and B. Yurke, *Phys. Rev. Lett.*, **81**, 485 (1998).
- [13] H. Flyvbjerg, T.E. Holy and S. Leibler, *Phys. Rev. Lett.*, **73**, 2372 (1994).
- [14] H. Flyvbjerg, T.E. Holy and S. Leibler, *Phys. Rev. E* **54**, 5538 (1996) .
- [15] H. Flyvbjerg and E. Jobs, *Phys. Rev. E* **56**, 7083 (1997).
- [16] E. Jobs, D. E. Wolf and H. Flyvbjerg, *Phys. Rev. Lett.* **79**, 519 (1997).
- [17] B. Houchmanzadeh and M. Vallade, *Phys. Rev. E*, **53**, 6320 (1996).
- [18] D. J. Bicout, *Phys. Rev. E* **56**, 6656 (1997).
- [19] D. J. Bicout and R. J. Rubin, *Phys. Rev. E* **59**, 913 (1999).
- [20] K. F. Freed *Phys. Rev. E*, **66**, 061916 (2002).
- [21] M. Hammele and W. Zimmermann, *Physical Review E*, **67**, 021903 (2003).
- [22] B. Perez-Ramirez, J.M. Andreu, M.J. Gorbunoff and S.N. Timasheff, *Biochemistry*, **35**, 3277-3285 (1996).
- [23] A. Vandecandelaere, S. R. Martin, M. J. Schilstra and P. M. Bayley, *Biochemistry*, **33**, 2792 (1994).
- [24] A. Vandecandelaere, S. R. Martin and Y. Engelbroghs, *Biochem. J.*, **323**, 189 (1997).
- [25] J. R. Peterson and T. J. Mitchison, *Chemistry and Biology*, **9**, 1275 (2002).
- [26] M.A. Jordan and L. Wilson, *nature Reviews Cancer* **4**, 253 (2004).
- [27] J.J. Correia and S. Lobert, *Curr. Pharma. Design* **7**, 1213 (2001).
- [28] B.S. Govindan and W.B. Spilman, Jr., *Phys. Rev. E* **70**, 032901 (2004).
- [29] R.A. Walker, E.T. O'Brien, N.K. Pryer, M.F. Soboiero and W.A. Voter, *J. Cell Biol.* **107**, 1437 (1988).
- [30] There are some errors in the formulae in the ref.[20]; here we give the corresponding corrected expressions.
- [31] D. Panda, M.A. Jordan, K.C. Chu and L. Wilson, *J. Biol. Chem.* **271**, 29807 (1996).